Tellus (1982), 34, 526–539

Available potential energy in the northern hemisphere during the FGGE year

By KYUNG DUCK MIN[1] and LYLE H. HORN, *Department of Meteorology, University of Wisconsin, Madison, Wisconsin 53706, U.S.A.*

(Manuscript received October 21, 1981; in final form March 3, 1982)

ABSTRACT

Northern Hemispheric twice daily data from the First GARP Global Experiment (FGGE) year are used to compare available potential energy estimates obtained using the so-called exact (isentropic) form of the equations with two commonly used approximate (isobaric) forms. The two approximate forms, one using a fixed lapse rate and the other a lapse rate which varies in the vertical, overestimate the total available potential energy except in mid-summer.

The greatest difference between the exact and approximate forms is in the eddy term, which is considerably smaller in the approximate forms, especially in spring and summer. Partitioning the eddy term into its standing and transient components shows that in the exact form the standing component exceeds the transient term. This is in contrast to the approximate form in which the transient term is the larger in every month except July. The latitudinal and monthly variations of the standing and transient terms show different patterns, especially in the standing component. In the approximate form the latitude of maximum standing eddy values is near 60° N in winter but shifts equatorward to about 30° N and decreases in summer. While the exact form shows a weak winter maximum near 60° N, the dominant maximum develops near 20° N in spring and shifts poleward to about 30° N and increases in summer.

The hemispheric distribution of the vertically integrated grid point values from which the eddy available potential energy was calculated and the standard deviation of these twice daily values produce results which show that the exact form values better conform to the pattern of cyclone activity than the approximate form. In general, the results indicate that the exact form of the available potential energy equations should be more extensively used in diagnostic work.

1. Introduction

It has been long recognized that the atmosphere's kinetic energy is obtained from its vast reservoir of gravitational potential and internal energies, the sum of which is commonly called the total potential energy. Because only a very small portion of the total potential energy can be converted to kinetic energy, it is highly desirable to separate that portion which can become kinetic energy from that which cannot.

Lorenz (1955a, 1967) defined available potential energy as the difference between the total potential energies of some initial atmospheric state and a reference state achieved through an adiabatic redistribution of mass to a horizontally stratified, statically stable state. In his formulation Lorenz (1955a, 1967) initially used an isentropic framework, but then noted that because most meteorologists think in terms of pressure as a vertical coordinate rather than potential temperature, there is an advantage in expressing the results in an isobaric framework. To do so he assumed that isentropic and isobaric surfaces do not differ greatly in their inclination to the horizontal. He noted that although the isobaric approximate form is convenient in interpreting the concept of available potential energy, future theoretical work should employ the exact form (i.e., isentropic formulation). Since Lorenz (1955a) most diagnostic studies have employed the approximate formulation. In fact all of the studies involving hemispheric or global calculations of the amounts

[1] Present affiliation: Department of Earth Science, Kyungpook National University Taegu 635, Korea.

 © 1982 Munksgaard, Copenhagen

of available potential energy have employed some type of approximate form. It has also become the basis of the description of the energy cycle in quasi-geostrophic theory (Holton, 1979). For estimates using the approximate form see, for example, Oort (1964), Oort and Peixoto (1974), Peixoto and Oort (1974), Oort and Peixoto (1976). Newell *et al.* (1974) used a somewhat different version of the approximate form in their global study of the amount of available potential energy.

The work of Dutton and Johnson (1967) brought renewed attention to the available potential energy equations in their so-called exact (isentropic) form, although Lorenz (1955b) in an earlier, less known work had maintained the equations in their exact formulation. Smith (1969) employing pressure coordinates also obtained an exact form. Recently Lorenz (1978) introduced the concept of moist available energy in which latent heat is included. However, in this paper our focus is on the more traditional "dry" available potential energy, which henceforth will be referred to as APE.

With respect to calculations involving the exact form, Dutton and Johnson (1967) estimated APE along the 75° W meridian for one year, while Smith and Horn (1969) used the exact form in pressure coordinates to estimate the contribution of APE over North America to the global APE for one month. Other studies using the exact form have examined the climatological generation of available potential energy in limited areas. Min and Horn (1974) and Rose (1976) estimated the generation due to sensible and latent heating, respectively for the east coasts of North America and Asia. Still others have studied the generation in storm volumes (Hahn and Horn, 1969; Johnson, 1970; Gall and Johnson, 1971; Bullock and Johnson, 1971, 1972; Wei, 1979). None have dealt with hemispheric or global domains.

In this paper, the available potential energy is calculated for the Northern Hemisphere using the exact isentropic form. Twice daily values are calculated for the period of the First GARP Global Experiment (FGGE) year 1 December 1978–30 November 1979. As in most previous studies, the APE is partitioned into its zonal and eddy parts. The eddy APE is further partitioned into standing and transient components. Also the geographical distribution of the vertically integrated grid point data used to calculate the eddy APE is related to observed cyclone activity.

The hemispheric results obtained using the exact form are compared with estimates based on two versions of the approximate form. One version employs the fixed static stability of the standard atmosphere, while the second allows the static stability to vary vertically in 50 mb increments. The comparisons reveal rather striking differences between estimates based on the approximate and exact forms. The differences involve the amounts of both the zonal and eddy APE, their seasonal trends and their geographical distributions.

2. The data set

In order to compare available potential energy estimates obtained using the approximate and exact forms of the equations over the Northern Hemisphere, it is important to use a data set that provides the most complete hemispheric coverage possible and is of excellent quality. Gridded data sets prepared twice daily by the National Meteorological Center (NMC) of the U.S. National Weather Service were used. In September 1978, in preparation for the FGGE year, NMC switched from the Hough spectral analysis (Flattery, 1970) to optimum interpolation (Bergman, 1978, 1979; McPherson *et al.*, 1979). An improvement in certain characteristics of the NMC gridded data apparently occurred at this time. Townsend (1980), who conducted a diagnostic study of the zonally averaged circulation, found that the NMC gridded data prior to September 1978 contained numerous superadiabatic layers and zonally averaged meridional winds which were virtually zero at all latitudes and all elevations. However, following the switch to optimum interpolation he noted a marked reduction in the number of superadiabatic layers and obtained zonally averaged winds which contained ageostrophic components. Consequently, he used the NMC gridded data for the FGGE year. This same basic data set is used for the available potential energy calculations of this study.

The FGGE level IIIa data set extends from December 1, 1978 through November 30, 1979. Because of the international effort made during the FGGE year to obtain a superior data set, the data used here were the best available at the time of the initiation of this study. These data were derived from a heterogeneous observing system (Fleming *et al.*, 1979a, b) using a global data assimilation system based on the method of optimum interpolation (McPherson *et al.*, 1979; Bergman, 1979). The data were available at 0000 and 1200 GMT on a 2.5° latitude-longitude grid for 12 mandatory levels. Of the 730 possible observation periods, 703 were available from NMC. However, in this study two additional time periods were eliminated because of suspect data, reducing the data sample to 701 time periods.

The hemispheric isentropic data were generated by Townsend (1980) through vertical interpolation of the mandatory level isobaric data to isentropic surfaces using an algorithm developed by Thomas Whittaker of the University of Wisconsin (1970, personal communication). In this algorithm pressure and all other parameters are assumed to vary linearly with $\theta^{1/\kappa}$.

A total of 16 isentropic levels with a 10 K vertical resolution were obtained starting from as low as 220 K and extending to at least 370 K. A horizontal resolution consisting of a 5° latitude–longitude grid was used. Before these vertical and horizontal resolutions were chosen, test calculations of the hemispheric available potential energy using different resolutions were made for one time period. The results are shown in Table 1. Note that a decrease in horizontal resolution from a 2.5° to 5° latitude–longitude grid produced practically no differences in the APE. On the other hand, decreasing the vertical resolution from 5 K to 10 K resulted in slightly larger APE values, particularly the zonal available potential energy. Note, however that there was very little change in the eddy available potential energy. It was decided

Table 1. *An example from 0000 GMT January 1, 1979 of calculations of APE using the exact isentropic form with different horizontal and vertical resolutions. D is the percentage difference. Units: 10^5 J m^{-2}*

Resolution		A	A_Z	A_E
Horizontal	2.5° lat.–long.	54.4	34.3	20.2
(vertical 10 K)	5.0° lat.–long.	54.6	34.2	20.4
	D (%)	0.4	−0.3	1.0
Vertical	5 K	51.3	31.2	20.0
(horizontal 2.5°)	10 K	54.4	34.2	20.2
	D (%)	5.7	8.8	1.0

to employ the 10 K resolution because of substantial savings in computing costs and because of the fact that the 10 K interval produced 16 isentropic levels from a total of 12 isobaric levels. To obtain 33 isentropic levels (5 K interval) from 12 isobaric levels would have been somewhat unrealistic.

3. Equations and computational methods

3.1. *Equations of APE in exact form*

Lorenz (1955a) defined available potential energy as the difference between the total potential energy in an initial state and a reference state which is achieved through an adiabatic redistribution of mass to a horizontally invariant, statically stable state. In the initial state the total potential energy for the hemisphere is denoted Π_H, and in the reference state Π_{RH}. Thus the available potential energy (A) per unit area is

$$A = \Pi_H - \Pi_{RH}. \tag{1}$$

Lorenz partitioned A into zonal and eddy parts, where the zonal part (A_Z) and eddy part (A_E) are given by

$$A_Z = \Pi_{RZ} - \Pi_{RH} \tag{2}$$

$$A_E = \Pi_H - \Pi_{RZ}, \tag{3}$$

where Π_{RZ} is the total potential energy within the zonal reference state. Theoretically the total potential energy in the exact form employs an integral extending from $\theta = 0$ to infinity. However, it is impossible in practice to integrate using these limits. Therefore, in this study upper and lower boundary integral limits were used.

The total potential energy per unit area can be expressed as

$$\Pi_H = \frac{c_p}{g p_{00}^{\kappa}(1+\kappa)} \frac{1}{S} \left[\int_S \int_{\theta_s}^{\theta_t} p^{1+\kappa} d\theta dS + \int_S \left(\theta_s p_s^{1+\kappa} - \theta_t p_t^{1+\kappa} \right) dS \right], \tag{4}$$

where c_p is specific heat at constant pressure, g is gravitational acceleration, κ is the ratio of the gas constant (R_d) to c_p, p_{00} is 1000 mb, p is pressure, θ is potential temperature and S is hemispheric surface area and $dS = a^2 \cos \phi \, d\lambda \, d\phi$, where a is the radius of the earth, ϕ is latitude, λ is longitude.

The s subscript denotes a value at the earth's surface and the t subscript denotes a value at the top of the volume of atmosphere. Likewise, the total potential energy in the hemispheric reference state is

$$\Pi_{\mathrm{RH}} = \frac{c_\mathrm{p}}{g p_{00}^{\kappa}(1+\kappa)} \frac{1}{S} \left[\int_S \int_{\theta_{\mathrm{RHs}}}^{\theta_{\mathrm{RHt}}} p_{\mathrm{RH}}^{1+\kappa} \, \mathrm{d}\theta \, \mathrm{d}S + \int_S \left(\theta_{\mathrm{RHs}} p_{\mathrm{RHs}}^{1+\kappa} - \theta_{\mathrm{RHt}} p_{\mathrm{RHt}}^{1+\kappa} \right) \mathrm{d}S \right]. \tag{5}$$

While θ_{RHt} is set equal to θ_t, θ_{RHs} is not necessarily equal to θ_s at a given point after the adiabatic redistribution of mass. Therefore, Π_H and Π_{RH} are computed separately. The hemispheric APE per unit area is then found using (1).

The total potential energy for the zonal reference state (Π_{RZ}) is obtained using eq. (5) but with the p_{RH} and θ_{RH} values replaced with p_{RZ} and θ_{RZ} which represent values within 5° zonal rings. Values of the total, zonal and eddy APE can be obtained by substituting Π_H, Π_{RH} and Π_{RZ} into eqs. (1) through (3).

The above equations require the evaluation of both a hemispheric reference pressure (p_{RH}) and a zonal reference pressure (p_{RZ}). For this study lower and upper boundary limits of 220 K and 370 K were used. The 370 K isentropic surface is usually near 150 mb, which is at about the level where the isentropic surfaces are quasi-horizontal. The reference pressures were calculated for 10 K intervals between 220 and 370 K, with the hemispheric (p_{RH}) and zonal (p_{RZ}) reference pressures calculated separately. In the free atmosphere where isentropic surfaces do not intersect the ground, the reference pressure is the area averaged pressure on a θ surface. However, nearer the earth's surface the effects of surface topography must be considered in obtaining reference pressures. In this study, an iterative method developed by Koehler (1979) was used. Koehler's method, although derived independently, is similar to that proposed by Taylor (1979). The method begins by calculating the area average pressure on each θ surface between θ_t and θ_0, the minimum surface θ value. These average pressures are then compared to the lowest observed surface pressure (p_{smin}). On all θ surfaces which do not intersect the ground, the reference pressure is set equal to the average pressure. On the remaining θ surfaces which intersect the ground, the iterative approach is employed.

It is instructive to partition the exact form of A_E into its standing and transient parts. Since twice daily APE values were computed in this study, the transient component of eddy APE ($\overline{A}_{\mathrm{Etr}}$) may be defined as

$$\overline{A}_{\mathrm{Etr}} = \overline{A}_\mathrm{E} - \overline{A}_{\mathrm{Est}} \tag{6}$$

where the overbar represents a monthly mean. Thus $\overline{A}_\mathrm{E}$ is the monthly mean of the twice daily values of A_E. The subscripts tr and st represent the transient and standing components, respectively. $\overline{A}_\mathrm{E}$ is given by

$$\overline{A}_\mathrm{E} = \overline{\Pi_\mathrm{H} - \Pi_{\mathrm{RZ}}}. \tag{7}$$

In common meteorological parameters the standing component of the eddy APE is given by

$$\begin{aligned} \overline{A}_{\mathrm{Est}} = {} & \frac{c_\mathrm{p}}{g p_{00}^{\kappa}(1+\kappa)} \frac{1}{S} \left[\int_S \int_{\theta_\mathrm{s}}^{\theta_\mathrm{t}} \overline{p}^{1+\kappa} \, \mathrm{d}\theta \, \mathrm{d}S + \int_S (\overline{\theta}_\mathrm{s} \overline{p}_\mathrm{s}^{1+\kappa} - \overline{\theta}_\mathrm{t} \overline{p}_\mathrm{t}^{1+\kappa}) \, \mathrm{d}S \right] \\ & - \frac{c_\mathrm{p}}{g p_{00}^{\kappa}(1+\kappa)} \frac{1}{S} \left[\int_S \int_{\theta_{\mathrm{RZs}}}^{\theta_{\mathrm{RZt}}} \overline{p}_{\mathrm{RZ}}^{1+\kappa} \, \mathrm{d}\theta \, \mathrm{d}S + \int_S (\overline{\theta}_{\mathrm{RZs}} \overline{p}_{\mathrm{RZs}}^{1+\kappa} - \overline{\theta}_{\mathrm{RZt}} \overline{p}_{\mathrm{RZt}}^{1+\kappa}) \mathrm{d}S \right] \end{aligned} \tag{8}$$

The computations for the standing terms were conducted using monthly mean surface pressure ($\overline{p}_\mathrm{s}$), and surface potential temperature ($\overline{\theta}_\mathrm{s}$).

3.2. *Equations of APE in approximate form*

The hemispheric results obtained using the exact form of the APE equations described in the previous section will be compared with the approximate form. Following Lorenz (1955a, 1967) the approximate form of the APE equations in isobaric coordinates are

$$\hat{A} = \frac{1}{2} \frac{c_\mathrm{p}}{g} \frac{1}{S} \int_S \int_p \{\Gamma_\mathrm{d}(\Gamma_\mathrm{d} - \tilde{\Gamma})^{-1} \tilde{T}^{-1} \tilde{T}''^2\} \mathrm{d}p \, \mathrm{d}S \tag{9}$$

$$\hat{A}_\mathrm{Z} = \frac{1}{2} \frac{c_\mathrm{p}}{g} \frac{1}{S} \int_S \int_p \{\Gamma_\mathrm{d}(\Gamma_\mathrm{d} - \tilde{\Gamma})^{-1} \tilde{T}^{-1} [T]''^2\} \mathrm{d}p \, \mathrm{d}S \tag{10}$$

$$\hat{A}_\mathrm{E} = \frac{1}{2} \frac{c_\mathrm{p}}{g} \frac{1}{S} \int_S \int_p \{\Gamma_\mathrm{d}(\Gamma_\mathrm{d} - \tilde{\Gamma})^{-1} \tilde{T}^{-1} T^{*2}\} \mathrm{d}p \, \mathrm{d}S \tag{11}$$

where the $\hat{}$ is used here to distinguish the approximate form from the exact form, Γ_d is the dry adiabatic lapse rate, $\tilde{\Gamma}$ is the hemispheric average of Γ on an isobaric surface, $\tilde{T}$ is the average of T on an isobaric surface, $[T]$ is the zonally averaged temperature on an isobaric surface and T^* is the deviation of temperature from its zonal mean. Thus $T^* = T - [T]$ represents the temperature deviation from its zonal mean. Likewise $T'' = T - \tilde{T}$ is the temperature deviation from the hemispheric mean, and $[T]'' = [T] - \tilde{T}$ is the temperature deviation of a zonal mean temperature from the hemispheric mean. Thus $\hat{A}_Z$ is determined by the variance of zonally averaged temperature and $\hat{A}_E$ by the variance of temperature within zonal rings. It should be emphasized that all the variables are calculated on isobaric surfaces. In this study the calculations extended vertically to the 150 mb surface which is near the 370 K surface used in the exact form calculations.

Using the approximate form of the equation, the standing and transient components of A_E are calculated in a manner similar to (6). The standing and transient $\hat{A}_E$ are expressed as

$$\overline{\hat{A}}_{Etr} = \overline{\hat{A}}_E - \overline{\hat{A}}_{Est} \tag{12}$$

where

$$\overline{\hat{A}}_E = \frac{1}{2}\frac{c_p}{g}\frac{1}{S}\int_S\int_p \overline{\gamma T^{*2}}\,\mathrm{d}p\,\mathrm{d}S \tag{13}$$

$$\overline{\hat{A}}_{Est} = \frac{1}{2}\frac{c_p}{g}\frac{1}{S}\int_S\int_p \bar{\gamma}\overline{T^{*2}}\,\mathrm{d}p\,\mathrm{d}S \tag{14}$$

where $\gamma = \Gamma_d(\Gamma_d - \tilde{\Gamma})^{-1}\,\tilde{T}^{-1}$.

4. Hemispheric estimates using the exact and approximate forms

Because a major goal of this investigation is to intensively examine the Northern Hemisphere supply of APE during the FGGE year, it is logical to begin by comparing the hemispheric results obtained using the two versions of the approximate form with those achieved from the exact form. In calculating the approximate form, the lapse rate was calculated in two ways: (1) a *fixed* lapse rate of the standard atmosphere (6.5 °C km^{-1}) and (2) a *variable* lapse rate which is allowed to vary between 50 mb increments of pressure. (However, note that a hemispheric *mean* value is used within each 50 mb increment.) Hereafter, the two versions of the approximate form will be referred to as the *fixed approximate* and *variable approximate* forms, respectively.

By employing the same data in calculating both the exact and approximate forms, any ambiguity which may arise in comparing results from different periods or areas is avoided. While most attention is given to intercomparisons based on the FGGE data calculations of this study, comparisons with results obtained by investigators using the approximate form for different data periods will also be briefly discussed.

4.1. *Time series of twice daily values of APE*

Twice daily values of total, zonal and eddy APE estimated using the FGGE level IIIa data from December 1, 1978 through November 30, 1979 are presented in Fig. 1. The estimates were obtained using the two versions of the approximate form and the exact form. The fixed approximate APE, presented in Fig. 1a, has the largest total and zonal values of the three forms. Its seasonal trend is almost entirely determined by the zonal APE ($\hat{A}_Z$). The variable approximate form (Fig. 1b) shows a similar trend but with the magnitudes of $\hat{A}$ and $\hat{A}_Z$ about 20% smaller than the fixed approximate form in the winter and about the same magnitude in summer. The exact form (Fig. 1c) exhibits smaller values of the total APE than either of the approximate forms except in mid-summer when it is about equal or slightly larger. These relative sizes and seasonal trends of total APE are similar to those obtained by Dutton and Johnson (1967), who used data from only the 75th meridian. Although Dutton and Johnson argued that the approximate forms overestimate the total APE through most of the year, there was some question as to whether the 75th meridian was representative of the entire Northern Hemisphere. The hemispheric results for the total APE shown in Fig. 1 support their argument.

The sharp contrasts presented in Fig. 1 occur in the eddy terms. Both approximate forms have relatively small eddy values with a tendency for the winter values to slightly exceed the summer values. On the other hand, the exact form (Fig. 1c) has eddy values that are nearly twice those of the approximate form, with the largest values in late spring and summer, not winter. While in the

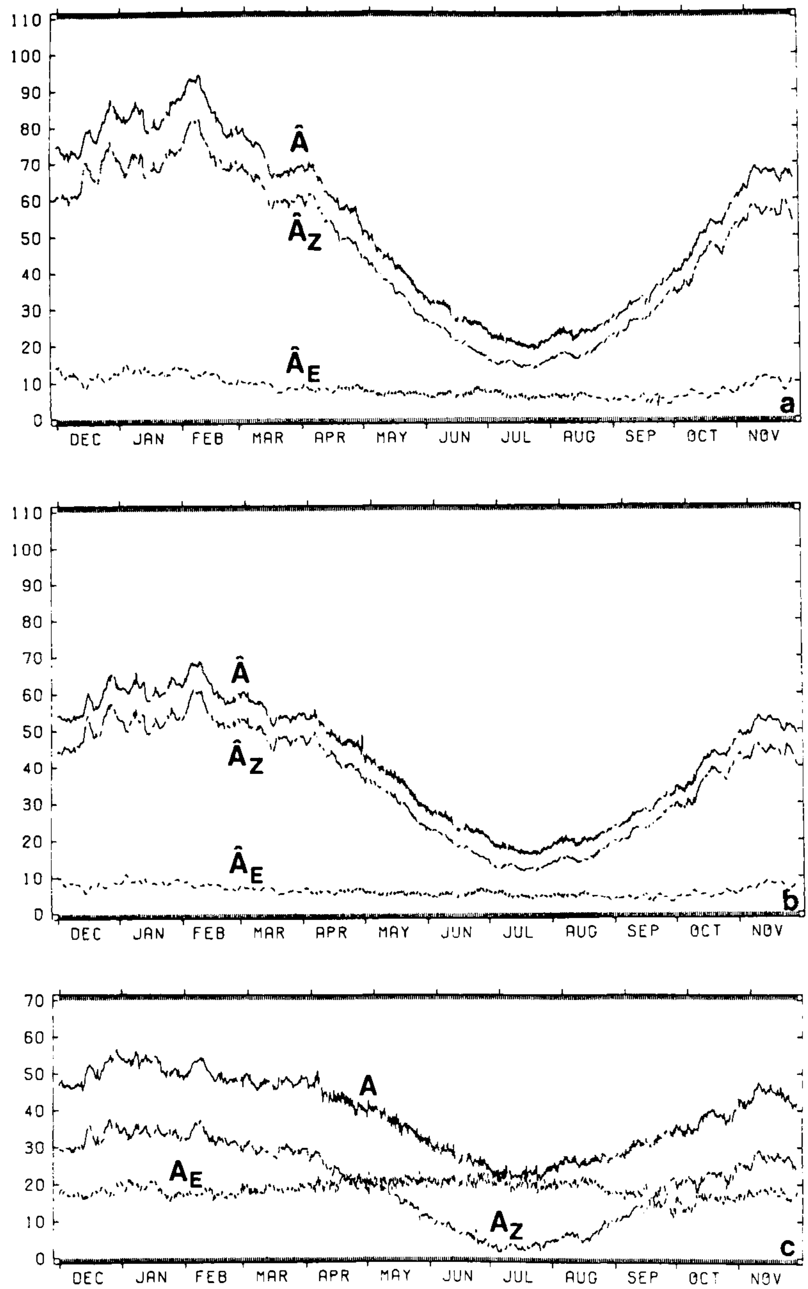

Fig. 1. Time series of twice daily APE values. Total (solid), zonal (dash-dot) and eddy (dash). (a) Fixed lapse rate approximate form. (b) Variable lapse rate approximate form. (c) Exact form. Units: 10^5 J m^{-2}.

approximate forms the eddy values are less than the zonal values throughout the year, in the exact form the eddy term exceeds the zonal term from May through September. In mid-summer the zonal term is very small. Peixoto and Oort (1974), using the approximate form with a variable lapse rate, note that the ratio of eddy APE to zonal APE is significantly larger in summer than winter (e.g. 0.19

in January versus 0.43 in July). In the exact form a similar but more dramatic trend exists (e.g. 0.50 in winter to about 4.0 in mid-summer).

Recall that the time series presented in Fig. 1 are based on twice daily data (0000 and 1200 GMT). A close inspection of the curves in this figure shows a tendency for a diurnal variation of APE which is most apparent in the exact form total APE from early April into mid-summer. The 1200 GMT values are larger than the 0000 GMT values. An examination of the APE calculated for various quadrants showed that nearly all of the contribution to the larger 1200 GMT values was provided by the large land masses, especially southern Asia and northern Africa during spring and summer. In these regions during this time of year the sun is high in the sky at 1200 GMT which favours warm surface temperatures and weak static stability.

The tendency for a greater diurnal variation in the exact form reflects a greater sensitivity of the exact form compared with the approximate forms. This greater sensitivity offers a major clue as to why the approximate and exact form results differ significantly. In the approximate form with a variable lapse rate, the lapse rate is allowed to vary from one 50 mb layer to another; however, hemispheric means of the lapse rate in each layer are used (e.g., the lapse rate used in the 950–900 mb layer is the same at 80° N latitude as at 20° N). In contrast, the exact (isentropic) form values are calculated at each grid point using the data at that grid point. The fact that the fixed lapse rate approximate form differs from the exact form even more than does the variable lapse rate form further suggests the significance of static stability in APE calculations. While vertical variation of the lapse rate brings this approximate form closer to the exact form, the hemispheric wide averaging probably robs it of the needed sensitivity to static stability variations.

In the approximate form the lack of sensitivity to static stability is probably most significant in the lower troposphere (below 700 mb) and also at high elevations (in this study between 250 and 150 mb). For example, in the first case, the winter lapse rate over the continental arctic and frozen Arctic Ocean commonly consists of an inversion from the surface to above 800 mb, while at the same time in the continental tropics the lapse rate in this layer is likely to be conditionally stable. The problem at high elevations results from the fact that in the tropical atmosphere the 250–150 mb layer is in the upper troposphere, where the lapse rate is only slightly less than dry adiabatic, while in polar regions the layer is in the lower stratosphere where the lapse rate is isothermal or less. Consequently, the stability factor which represents a mean of these diverse conditions is neither representative of the high tropical nor high polar atmosphere. When it is used in eqs. (9–11) to multiply the temperature variances in these regions, a bias is assured. At high elevations the problem is compounded by the fact that the temperature gradient above 200 or 250 mb reverses between winter and summer.

4.2. *Representativeness of the FGGE year*

A question can be raised regarding the representativeness of the FGGE year. Perhaps monthly means obtained from several years of data as was done by Oort and Peixoto (1976) would be advantageous in revealing the characteristics of the Northern Hemisphere APE. However, an examination of Table 1 of their study shows only relatively small year to year changes within their 5 year period. Further insight into the representativeness of the FGGE year results is presented in Table 2 which compares the 5 year mean monthly estimates of Peixoto and Oort (1974) with those obtained here. Both sets of values shown in Table 2 were achieved using the approximate form with a variable lapse rate. Considering the different data periods, the results from the two studies are quite similar. The slightly larger values obtained by

Table 2. *Comparisons of APE (approximate form, variable lapse rate) obtained in this study using FGGE year data with the five year means (in parentheses) obtained by Peixoto and Oort (1974). Units $10^5\ Jm^{-2}$*

	$\hat{A}$	$\hat{A}_Z$	$\hat{A}_E$
December	57.2 (63.0)	49.3 (53.7)	8.0 (9.3)
January	61.6 (66.3)	52.5 (55.8)	9.0 (10.5)
February	62.6 (65.9)	54.9 (56.4)	7.7 (9.5)
March	55.8 (61.9)	49.2 (53.6)	6.6 (8.2)
April	49.6 (49.3)	43.3 (42.4)	6.3 (6.9)
May	36.6 (36.8)	31.0 (30.3)	5.6 (6.5)
June	24.5 (24.7)	19.0 (18.8)	5.4 (5.9)
July	17.7 (18.6)	12.8 (13.0)	4.9 (5.6)
August	20.3 (20.1)	15.5 (15.0)	4.8 (5.1)
September	27.7 (29.4)	23.5 (23.8)	4.2 (5.6)
October	40.0 (42.0)	34.8 (35.0)	5.1 (6.9)
November	51.1 (54.9)	43.7 (46.3)	7.4 (8.6)
Average	42.1 (44.4)	35.8 (37.0)	6.3 (7.4)

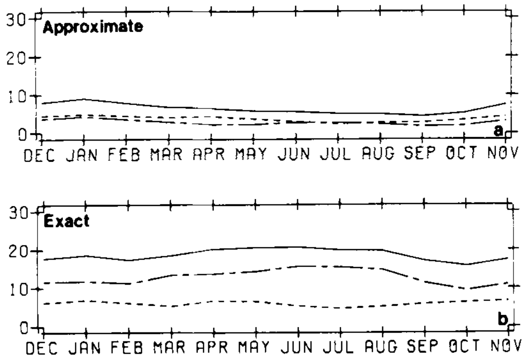

Fig. 2. Northern Hemisphere eddy APE (solid) partitioned into standing eddy (dash-dot) and transient eddy (dash). (a) Variable approximate form. (b) Exact form. Units 10^5 J m^{-2}.

Peixoto and Oort probably reflect the fact that their isobaric calculations extended to 50 mb, while ours only extend to 150 mb. The contribution from the 150–50 mb layer is usually relatively small thus probably accounting for the only slightly larger values obtained by Peixoto and Oort.

4.3. *Standing and transient components of eddy APE*

Further insight into the basic differences between the approximate and exact forms of the eddy APE was achieved by partitioning the term into its standing and transient components using eqs. (6–8) and (12–14). This partitioning is similar to that done by Peixoto and Oort (1974). Monthly means calculated from the twice daily values are shown in Fig. 2. Not only is A_E (exact form) considerably larger than $\hat{A}_E$ (approximate form) but the relative magnitudes of the standing and transient components are reversed. In the variable approximate form (Fig. 2a) the transient component slightly exceeds the standing component in every month except July. This is in qualitative agreement with the results of Peixoto and Oort (1974) who obtained monthly mean transient terms which exceed the standing terms for every month of the year. In contrast to the variable approximate form, the exact form yields standing eddy components which exceed the transient values for all months, with the largest differences in summer (Fig. 2b).

To better interpret the behaviour of the standing and transient components of eddy APE, graphs showing these components as a function of time and latitude were prepared for both the variable approximate and exact forms. Contributions from each zonal ring (weighted for the area of the ring) were plotted for each month. In the approximate form (Fig. 3a), the main contribution of the standing eddy term comes from the region between 55° and 65° N in winter but shifts equatorward to near 30° N in summer. The heavy line is drawn through regions of maximum contribution. Not only is there a southward shift in regions of maximum contribution, but the values decrease from about 13 × 10^5 J m^{-2} in winter to 5 × 10^5 J m^{-2} in summer. This equatorward shift of the primary contribution might be interpreted as reflecting the larger east–west temperature contrasts between oceans and continents in higher

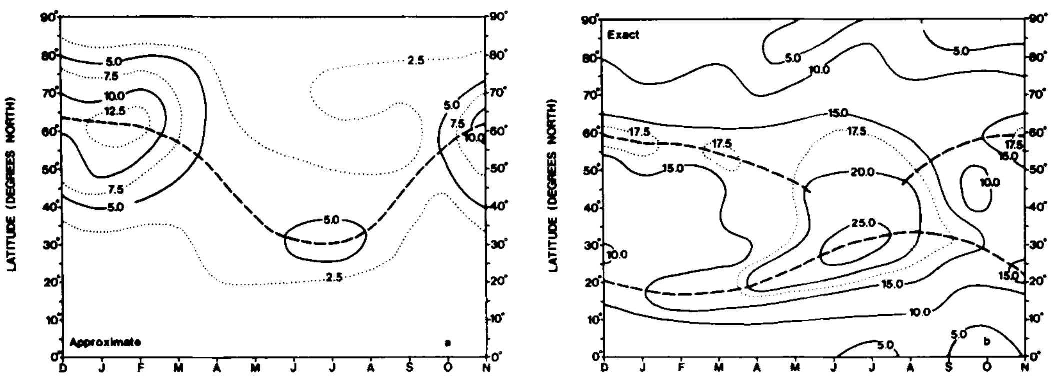

Fig. 3. Standing eddy APE as a function of month and latitude. Heavy dashed lines drawn through zones of maximum values. (a) Variable approximate form. (b) Exact form. Units 10^5 J m^{-2}. Note in (b) isopleths are drawn for only 5 × 10^5 J m^{-2} intervals, except a 17.5 × 10^5 J m^{-2} isopleth (dotted) is added to better reveal the northern maximum.

latitudes in winter, but in the subtropics in summer. However, by summer the contrasts have weakened.

The graph showing the exact form of the standing eddy APE as a function of latitude and month (Fig. 3b) provides a significantly different pattern from that for the approximate form. In winter the largest standing eddy values are located at 55–65° N, near their position in the approximate form, but with the exact form maximum less pronounced. There is also an indication of a weaker secondary winter maximum near 20° N. During spring and summer this southern maximum becomes strongly dominant, with the largest standing eddy values shifting poleward to about 30° N and increasing to 25×10^5 J m^{-2} by early summer. This maximum is five times greater than the summer values for the approximate form and twice as large as the winter maximum of the approximate form. The heavy dashed lines on Fig. 3b approximately describe the seasonal shifting of the zones of the two maxima. While the northern maximum, which has characteristics similar to that of the approximate form, is evident during the cooler seasons, it is the southern maximum which is clearly dominant through most of the year.

The pattern displayed in Fig. 3b can be explained in terms of continent–ocean contrasts. As in the case of the approximate form (Fig. 3a), the winter maximum, although not pronounced, probably reflects the east–west contrast between cold continents and warmer subpolar oceans. In the case of the southern maximum, its poleward shift and intensification likely result from the northward movement of the sun. As spring and summer approach the thermal contrast between the subtropical continents and oceans increases, particularly at the surface and in the low troposphere. At the same time static stability over the continents weakens considerably while the stability over the oceans experiences a much smaller change. These factors, of course, are consistent with the development of the monsoon circulations in the subtropics.

The transient eddy component as a function of latitude and month is shown in Fig. 4. In the approximate form, slightly larger values occur in winter than in summer, as would be expected (Fig. 4a). The zone of maximum contribution is between 50° and 55° N in winter shifting to 55°–60° N in mid-summer. The exact form results displayed in Fig. 4b show values which are generally somewhat larger than the approximate form in middle and high latitudes and considerably larger in low latitudes. In the exact form the zone of maximum contribution shifts southward from 40–45° N in early winter to 35–40° N in late winter and early spring and then poleward to 50°–55° N in summer. It is interesting to note that the maximum contributions from the exact form are located farther south than those from the approximate form and are thus located more closely to the zones of maximum cyclogenesis as found by Whittaker and Horn (1981) for North America and by Klein (1957) for the Northern Hemisphere. (Also see Fig. 3.11 in Palmen and Newton (1969) which includes some of Klein's data.) In late winter and early spring, a time of most frequent cyclogenesis, the latitudes of maximum transient eddy APE (exact form) and cyclogenesis nearly coincide. However, at other times of the FGGE year the maximum

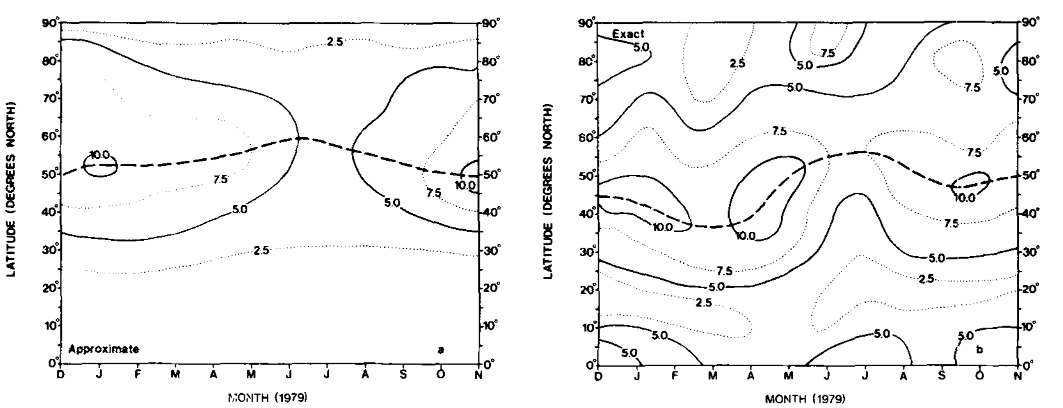

Fig. 4. Transient eddy APE as a function of month and latitude. Heavy dashed lines drawn through zones of maximum values. (a) Variable approximate form. (b) Exact form. Units 10^5 J m^{-2}.

values of transient APE were located somewhat farther north than the long term values of most frequent Northern Hemisphere cyclogenesis. Nevertheless, the fact that the exact form transient eddy APE agrees better than the approximate form with the latitudes of maximum cyclogenesis provides support for use of the exact form in studies which relate cyclone activity to available potential energy.

4.4. *Geographical distribution of hemispheric grid point data and their standard deviations*

Although APE determinations require integration over an area (APE is not defined at individual grid points), and examination of the distribution of the grid point values offers additional insight into the differences between the approximate and exact forms of APE. in this study maps were prepared showing the winter season (DJF) geographical distributions of the vertically integrated grid point values from which the eddy APE was calculated. Because vertical integration was employed the values were expressed in specific units (J kg^{-1}). This was necessary because in the approximate form the mass between 1000 and 150 mb is fixed, but in the exact form the mass between θ_s and θ_t can vary from point to point. In viewing Fig. 5a it should be kept in mind that because the approximate form is calculated using the quadratic of temperature deviations, all grid point values will be positive (or zero). On the other hand, as shown in Fig. 5b, the exact form grid point values can be either positive or negative although their integral within a zonal ring is positive.

The distribution of grid point values for the variable lapse rate approximate form (Fig. 5a) shows a maximum over northeastern Asia, reflecting the large departures (cold) of the temperature in this region from the zonal mean. A secondary maximum is located over the Greenland–Iceland area with other maxima located in northeastern North America and the Alaskan regions. The exact form distributions shown in Fig. 5b are quite different from those of the approximate form. There are both positive and negative grid point values with the negative values found in regions where the isentropic surfaces are at low pressure (i.e., high elevation) and the positive values at high pressure (i.e., lower elevation) with respect to the zonal reference pressure. Considering only a zonal ring, the air parcels with negative values (relatively cold) would sink, while those with positive values (relatively warm) would rise in moving toward the reference state of the zonal ring. It is interesting that the center of negative values in Fig. 5b is displaced southeastward from the center noted in the approximate representation. This more southeasterly location is closer to both the cyclogenetic area off the east coast of Asia and the mean position of the Aleutian low. A second area of negative values is located over northeastern North America in a position similar to one of the maxima in the approximate form.

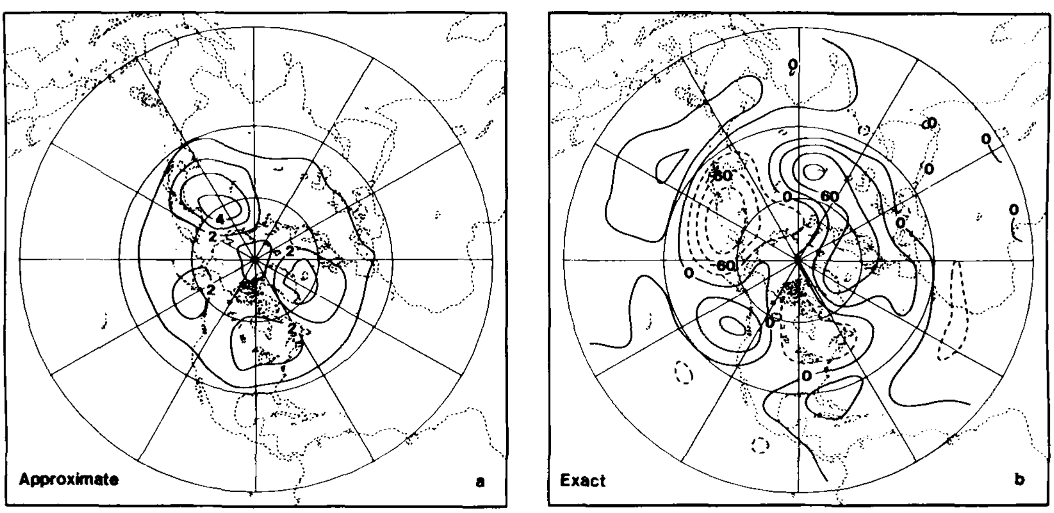

Fig. 5. Distribution of grid point values (10^2 J kg^{-1}) from eddy APE calculation for winter (DJF). (a) Variable approximate form. (b) Exact form.

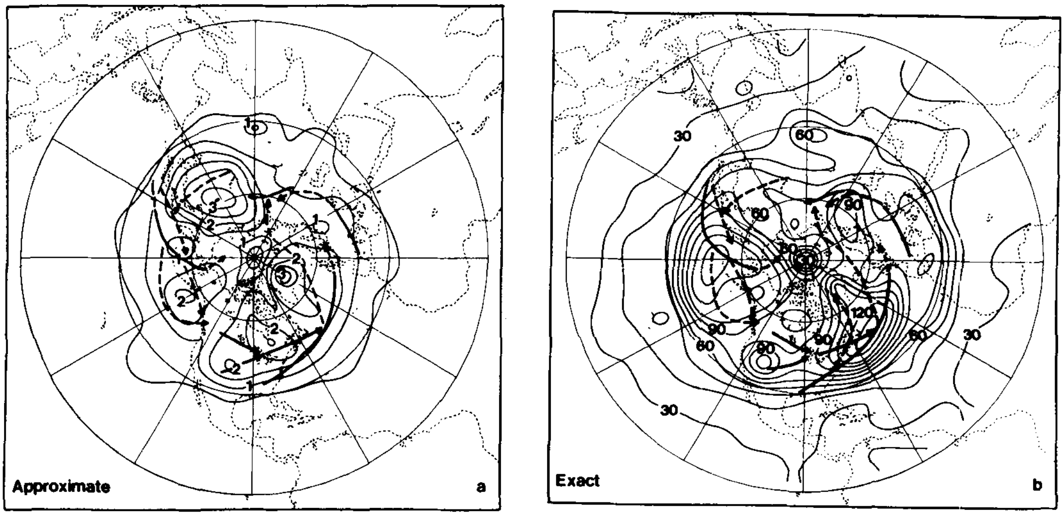

Fig. 6. Distribution of the standard deviations (10^2 J kg^{-1}) of the twice daily grid point values for winter (DJF). (a) Variable approximate form. (b) Exact form.

While the distributions of the grid point values of which the eddy APE is composed are of interest, the standard deviations of these twice daily values are of equal or greater interest. At a grid point the vertically integrated values fluctuate from day-to-day as cyclones move through the area. Thus the areas of larger standard deviations should more-or-less reveal the location of cyclone tracks. Consequently, we have superimposed the primary and secondary cyclone tracks for the FGGE year winter season (DJF) on the standard deviation fields (Fig. 6). The cyclone tracks were determined independently by Linda M. Whittaker (1981, personal communication) who was unfamiliar with the distribution of eddy APE grid point data and their standard deviations. In examining Fig. 6 it should be noted that much larger standard deviations occur in the exact form data than in the approximate form. Because it is quadratic in temperature, the approximate form grid point values are all positive; however, in the exact form the values range from large negative to large positive. Thus standard deviations calculated from the twice daily values should be much larger for the exact form data than for the approximate form.

In the approximate form (Fig. 6a) the maximum standard deviation is over the Greenland–Iceland area with a close secondary maximum over Siberia in the same location as the region of maximum grid point values of Fig. 5a. In contrast, the maximum standard deviation in the exact form is much larger and is located off the northeastern coast of North America with a secondary maximum positioned over the North Pacific near the southwestern Aleutian Islands (Fig. 6b). Both of these centers are located downstream from the centers of maximum eddy APE grid point data shown in Fig. 5b. An examination of the cyclone tracks superimposed on Fig. 6 shows a remarkably close relationship between cyclone tracks and the maximum standard deviations of grid point data obtained from the exact form (Fig. 6b), but a poor relationship between cyclone tracks and standard deviations obtained from the approximate form (Fig. 6a). Certainly, the results displayed in Fig. 6 add support for use of the exact form of APE when studying cyclone activity.

5. Summary and suggestions for future work

In this study, FGGE year data (December 1978–November 1979) were used to study the available potential energy over the Northern Hemisphere. Hemispheric values were obtained using two approximate forms (fixed and variable lapse rates in an isobaric framework) and the exact form in an isentropic framework. The available potential energy was partitioned into zonal and eddy parts, and the results expressed in time series of twice-daily values (0000 GMT and 1200 GMT). The eddy APE was divided into its standing and transient components. Additionally, the geographical distribution of the vertically integrated grid point values from which eddy APE was calculated and their standard deviations were examined. The following major results were obtained:

(1) Comparisons between the approximate and exact forms of the total APE calculations gave significantly different hemispheric results. The approximate forms, especially the form using a fixed lapse rate, significantly overestimated the total APE, except in mid-summer.

(2) The most striking difference between the approximate and exact forms was in the eddy APE values. Although the approximate form yields larger values of the total APE than the exact form, the eddy values from the exact form are about two to three times larger than those from the approximate form. While the approximate form of eddy APE shows a small seasonal variation with minimum values in summer, the exact form exhibits its largest eddy APE values in late spring and summer. This probably results from the strong land–ocean contrasts in the subtropics during these seasons of high sun and the greater sensitivity of the exact form to static stability. These larger late spring and summer eddy APE values are likely related to monsoon activity.

(3) A breakdown of the eddy APE into its standing and transient components produces very different results for the approximate and exact forms. In the approximate form, the transient eddy APE exceeds the standing eddy APE for all months except July. In contrast, in the exact form the standing component exceeds the transient component for every month. Charts, in which the monthly mean values of the standing components are plotted versus latitude, show that in the approximate form the maximum values move toward lower latitudes (near 30° N) and decrease in value as summer approaches. In the exact form the standing eddy values are not only larger, but show a different seasonal variation. Although a weak winter maximum is found at about the same latitude as in the approximate form, the dominant feature of the exact form is the maximum which appears at low latitudes (near 20° N) in early spring and shifts slightly poleward to about 30° N and increases as summer approaches. The summer values from the exact form are five times as large as those in the approximate form. These large standing eddy values and their seasonal displacement appear to support their relationship to monsoon activity.

In contrast to the standing eddy APE values, the transient eddy values show less difference between the approximate and exact forms. The latitude of maximum values for both the approximate and exact transient eddy values varies less with season than in the standing eddy case. The latitude of the maximum values obtained from the exact form is slightly farther south in late winter and spring than that of the approximate form. The latitude (35–40° N) and season of this maximum agrees well with the long term maximum of cyclogenesis.

(4) Hemispheric maps showing the distribution of the vertically integrated grid point data from which the eddy APE was calculated were prepared for winter and summer. The exact form distribution appears to agree better with the distribution of cyclogenetic regions than the approximate form. More significantly, the standard deviations of the twice daily vertically integrated values for the winter season have a pattern which remarkably agrees with the principal and secondary cyclone tracks during the FGGE year winter. On the other hand, the approximate form standard deviations show little relationship to the winter cyclone tracks. Results such as these and those noted above support the use of the exact form of the available potential energy equations in diagnostic work.

Although the above results show pronounced differences between calculations based on the exact and approximate forms, we should again note that the approximate form has been used for more than twenty years in diagnostic studies, especially those involving the energetics of the entire hemisphere or globe. Certainly the approximate form is self-consistent and constitutes a description of the energy cycle in terms of temperature variance (rather than available potential energy). Because of its long history and because it is easier to calculate than the exact form, the approximate form will likely be used in some future studies. We feel however, that it is important that the meteorological community be aware of the significant differences that exist between the approximate and exact form results. These differences not only involve the actual amounts of APE but also its seasonal variation.

In studying the energetics of the earth's atmosphere much additional work remains. This work should include studies of the temporal and spatial relationships between the exact form APE and extratropical cyclone activity. Further comparisons between the exact and approximate form APE values are in order. For example, the relationship between the observed kinetic energy and both forms of the APE should be examined. Likewise, comparisons between the hemispheric generation of APE obtained using the exact and approximate forms is needed. These later studies could be part of the major undertaking of the computation of the Northern Hemisphere energy cycle using the exact and approximate forms. Other studies might also be considered. For example, does the diurnal variation of APE somehow influence the most likely time of cyclogenesis? Meteorologists are fully aware of the importance of diurnal heating in producing thunderstorms and other meso-scale phenomena, but have given little thought to the larger scale. And finally, additional studies of the APE and its generation in various limited regions appear in order. We are initiating work into some of these problems.

6. Acknowledgements

The authors deeply appreciate the support provided by Dr. Thomas Koehler throughout much of this study, including the computational work, discussions concerning the basic approach and suggestions regarding the manuscript. The work of Dr. Ron Townsend and Thomas Whittaker in conducting the transformation of the FGGE data from isobaric to isentropic coordinates is sincerely acknowledged. The work of Linda Whittaker in providing cyclone track data and assisting with the final manuscript is much appreciated. We also thank Pat Marvin, Brian Jarvis, Kathi Marvin and Lans Rothfusz for their assistance with figures and data handling. Thanks are also due to Professors D. R. Johnson, J. E. Kutzbach and S. Hastenrath for their suggestions. Finally we thank Mrs Eva Singer for typing the final manuscript. The research was supported by NSF Grant ATM 7918761.

REFERENCES

Bergman, K. H. 1978. Role of observational errors in optimum interpolation analysis. *Bull. Am. Meteorol. Soc. 59*, 1603–1611.

Bergman, K. H. 1979. Multivariate analysis of temperature and winds using optimum interpolation. *Mon. Wea. Rev. 107*, 1423–1444.

Bullock, B. R. and Johnson, D. R. 1971. The generation of available potential energy by latent heat release in a mid-latitude cyclone. *Mon. Wea. Rev. 99*, 1–14.

Bullock, B. R. and Johnson, D. R. 1972. The generation of available potential energy by sensible heating in Southern Ocean cyclones. *Q. J. Roy. Meteorol. Soc. 98*, 459–518.

Dutton, J. A. and Johnson, D. R. 1967. The theory of available potential energy and a variational approach to atmospheric energetics. *Adv. Geophys. 12*, 333–433.

Flattery, T. W. 1970. Spectral models for global analysis and forecasting. *Proceedings of the Sixth AWS Technical Exchange Conference*, U.S. Naval Academy, Annapolis, Maryland, Air Weather Service Technical Report, 242, 42–54.

Fleming, R. J., Kaneskige, T. M. and McGovern, W. E. 1979a. The Global Weather Experiment I. The observational phase through the first special observing period. *Bull. Am. Meteorol. Soc. 60*, 649–659.

Fleming, R. J., Kaneskige, T. M., McGovern, W. E. and Bryan, T. E. 1979b. The Global Weather Experiment II. The second special observing period. *Bull. Am. Meteorol. Soc. 60*, 1316–1322.

Gall, R. L. and Johnson, D. R. 1971. The generation of available potential energy by sensible heating: A case study. *Tellus 23*, 466–482.

Hahn, D. G. and Horn, L. H. 1969. The generation of available potential energy in a mid-latitude cyclone. Studies of large scale atmospheric energetics. Final report ESSA grant WBG-52, University of Wisconsin, 1–56.

Holton, J. R. 1979. *An introduction to dynamic meteorology*. New York: Academic Press Inc., 250–260.

Johnson, D. R. 1970. The available potential energy of storms. *J. Atmos. Sci. 27*, 727–741.

Klein, W. H. 1957. Principal tracks and mean frequencies of cyclones and anticyclones in the Northern Hemisphere. Res. Pap. No. 40, U.S. Weather Bureau, U.S. Government Printing Office, Washington, D.C., 20402, 60 pp.

Koehler, T. L. 1979. A case study of height and temperature analysis derived from Nimbus 6 satellite soundings on a fine mesh grid. *Ph.D. thesis*. Department of Meteorology, University of Wisconsin-Madison, 162–182.

Lorenz, E. N. 1955a. Available potential energy and the maintenance of the general circulation. *Tellus 7*, 157–167.

Lorenz, E. N. 1955b. Generation of available potential energy and the intensity of the general circulation. *Large Scale Synoptic Processes*, University of California (Los Angeles), Department of Meteorology.

Lorenz, E. N. 1967. *The nature and theory of the general circulation of the atmosphere*, W.M.O., 161 pp.

Lorenz, E. N. 1978. Available energy and the maintenance of a moist circulation. *Tellus 30*, 15–31.

Min, K. D. and Horn, L. H. 1974. The generation of available potential energy by sensible heating along the east coasts of Asia and North America. *J. Meteorol. Soc. Japan 52*, 204–217.

McPherson, R. D., Bergman, K. H., Kistler, R. E., Rasch, G. E. and Gordon, D. S. 1979. The NMC operational global data assimilation system. *Mon. Wea. Rev. 107*, 1445–1461.

Newell, R. E., Kidson, J. W., Vincent, D. G. and Boer, G. J. 1974. *The general circulation of the tropical atmosphere and interaction with extratropical latitudes*, 2. The MIT Press, 371 pp.

Oort, A. H. 1964. On the estimates of the atmospheric energy cycle. *Mon. Wea. Rev. 92*, 483–493.

Oort, A. H. and Peixoto, J. P. 1974. The annual cycle of the energetics of the atmosphere on a planetary cycle. *J. Geophys. Res. 79*, 18, 2705–2719.

Oort, A. H. and Peixoto, J. P. 1976. On the variability of the atmospheric energy cycle within a 5-year period. *J. Geophys. Res. 81*, 21, 3643–3659.

Palmén, E. and Newton, C. 1969. *Atmospheric circulation systems*. New York: Academic Press Inc., p. 84.

Peixoto, J. P. and Oort, A. H. 1974. The annual distribution of atmospheric energy on a planetary scale. *J. Geophys. Res. 79*, 15, 2149–2159.

Rose, W. J. 1976. The generation of available potential energy by latent heating along the east coasts of Asia and North America. *M.S. thesis*, Department of Meteorology, University of Wisconsin-Madison, 83 pp.

Smith, P. J. 1969. On the contribution of a limited region to the global energy budget. *Tellus 21*, 202–207.

Smith, P. J. and Horn, L. H. 1969. A computational study of energetics of a limited region of the atmosphere. *Tellus 21*, 193–201.

Taylor, K. 1979. Formulas for calculating available potential energy over uneven topography. *Tellus 31*, 236–245.

Townsend, R. D. 1980. A diagnostic study of the zonally-averaged global circulation in isentropic coordinates. *Ph.D. thesis*. Department of Meteorology, University of Wisconsin-Madison, 221 pp.

Wei, Ming-Ying 1979. The energy budgets of a developing cyclone over the East China Sea during the 1975 Air Mass Transformation Experiment. The University of Oklahoma, Contribution No. 79–1, 136 pp.

Whittaker, L. M. and Horn, L. H. 1981. Geographical and seasonal distribution of North American cyclogenesis, 1958–1977. *Mon. Wea. Rev. 109*, 2312–2322.